PROSIDING SNTTM XXIII 2025
Volume 23, No. 1, Tahun 2025, 9 Oktober 2025
e-ISSN 2623-0313
p-ISSN 3032-1972

Aerodynamic effect of windbreak on the crosswind phenomenon on a high-speed train

Naufal P. Ramadhan[a] , Harinaldi[a,1]
[a]Mechanical Engineering Department, Faculty of Engineering, Universitas Indonesia, Depok, 16424
[1]Email korespondensi: harinald@eng.ui.ac.id

Abstract. Crosswind greatly affects the aerodynamic performance and operational safety of the high-speed train. Windbreak is one of the windproof facilities commonly used for high-speed trains in windy areas. This study aims to see how variations in windbreak height (3.8 m; 4.4 m; and 5.2 m) can affect the aerodynamic performance of high-speed trains. 3 aerodynamic coefficients (drag, lift, and rolling moment) of the HST were compared when the train passed the track under the same conditions using the ANSYS FLUENT CFD simulation. Sudden changes in aerodynamic loads are evident in the pressure contour visualization. First, the aerodynamic coefficient of the train will decrease significantly as it enters the windbreak. Second, the 'IN' process of the windbreak track has a larger aerodynamic load fluctuation than the 'OUT' process. Third, the height of the windbreak does not significantly change the trend of the aerodynamic coefficient graph; there is only a phase difference and the magnitude of the amplitude formed. The highest average drag and lift coefficients occur at a height of 5.2 m, with values of 0.29 and 0.011, respectively. Meanwhile, the highest average rolling moment coefficient occurs at a windbreak height of 3.8 m, with a value of 0.0028.

Keywords: crosswind; high-speed train; windbreak; aerodynamic coefficient

Received: 30 September 2025; **Presented:** 9 October 2025; **Publication:** 9 March 2026
DOI: https://doi.org/10.71452/xk93bt57

INTRODUCTION

Currently, the Jakarta-Bandung High-Speed Train operated by PT KCIC has become a popular mode of land transportation for the public, especially those with frequent travel between Jakarta and Bandung. To ensure the safety and comfort of its operation, high-speed trains must adapt to various situations. One of these is the crosswind effect, where at high speeds, the airflow over the train surface exhibits different characteristics across sections (Yao Shuanbao, 2013). The crosswind effect itself is a problem and challenge for high-speed trains. Under strong crosswinds, the train's aerodynamic performance decreases drastically, and the aerodynamic load experienced by the train increases rapidly. This affects the train's stability and even causes trains to derail and overturn (Yang et al., 2019; Baker et al., 2013). Based on statistics, from 1956 to 2000, there were a total of 26 serious train accidents caused by strong crosswinds that occurred in Xinjiang, China (Zhengyi Yao, 2012).

With the rapid development of high-speed rail infrastructure, windproof facilities, such as windbreaks and anti-wind open-cut tunnels (AOT) have been gradually applied along non-elevated tracks in windy areas to ensure the safety of railway traffic. Among the two facilities, windbreaks are the most frequently used. When a high-speed train is fully running in a windbreak, the influence of the crosswind on the train's aerodynamic loads becomes greatly reduced (Zhang et al., 2018; Guanxiong Liu, 2017). Research (Tomasini et al., 2014) shows that under crosswind conditions, different infrastructure scenarios display a diversity of flow and pressure structures.

Experimental methods and numerical simulations are generally used to view and analyze the aerodynamic performance of high-speed trains. Compared to experiments, numerical simulations can more efficiently obtain vehicle movement scenarios and other data in greater detail (Cheng et al., 2011). A study using these two methods was conducted to assess the influence of crosswind on high-speed trains. However, the maximum relative error between numerical simulations and experimental tests is only 5% (Yang et al., 2017). This suggests that numerical models could be a substitute for experimental tests in this study.

In this study, the author will analyze changes in aerodynamic conditions that occur on the track with a windbreak in a crosswind condition. The analysis is carried out by looking for the value of the aerodynamic coefficient at the time the train enters, passes through, and exits the windbreak construction. There are 2 aerodynamic forces and 1 moment to be analyzed, namely, lift force, drag force, and rolling moment, because these three values have a big role in the occurrence of an overturned train. In this research, the train model used was the CR400AF train which was designed using the Autodesk Inventor application based on photo analysis. Furthermore, a CFD numerical simulation will be carried out using the help of ANSYS FLUENT software to obtain aerodynamic coefficients and the process of high-speed train flow due to crosswind on the track with windbreak.

The purpose of this study is to analyze phenomena in the windbreak region in relation to the aerodynamic coefficients and pressure distributions that occur when a train crosses the track with windbreak infrastructure at 3 height variations. In the results of this study, we will get a value of 3 aerodynamic coefficients such as rolling moment, lift force, and drag force starting from entering to exiting the windbreak track.

PROSIDING SNTTM XXIII 2025
Volume 23, No. 1, Tahun 2025, 9 Oktober 2025
e-ISSN 2623-0313
p-ISSN 3032-1972

METHODOLOGY

Geometry and Boundary Conditions

The simulation research in this study uses a 1:20 scale of the actual dimensions. This scaling is done due to limited computational capabilities as well as shortening the simulation time using ANSYS Fluent. In this case, the value of (Re) generated is already very large (Deng et al. 2019b; Deng et al. 2020; Niu et al. 2019; Chen et al. 2016). There is a condition of self-modelling region flow. This is a phenomenon where when (Re) is in a certain range of values, the flow and distribution of speed become comparable and do not depend on (Re) conditions. The flow field can be said to be in the self-modelling region zone because it is already in a very turbulent condition. In this study, the value of Re was as large as 10^6. Therefore, the train's speed in the simulation can be equated to the real-world speed of 350 km/h.

A model of the High-Speed Train CR400AF was developed by analysing 2D photos of the side, front, and top views collected. The designed train will only have 2 locomotives and 1 carriage because it has presented the train parts, namely the nose, body, and the tail of the train (Yang et al., 2018). The total length of the train is 79.4 m with a locomotive 27.2 m long and a train body 25 m long (KCIC, 2020). Train models are simplified, such as windowless, pantograph, bogie, etc. this is done to obtain better efficiency because the use of windows and other details has little effect on the simulation (Niu et al., 2018). The model is shown in Fig.1

Fig. 1 Comparison between the (a) real CR400AF train and (b) 1:20 simplified model for numerical simulation.

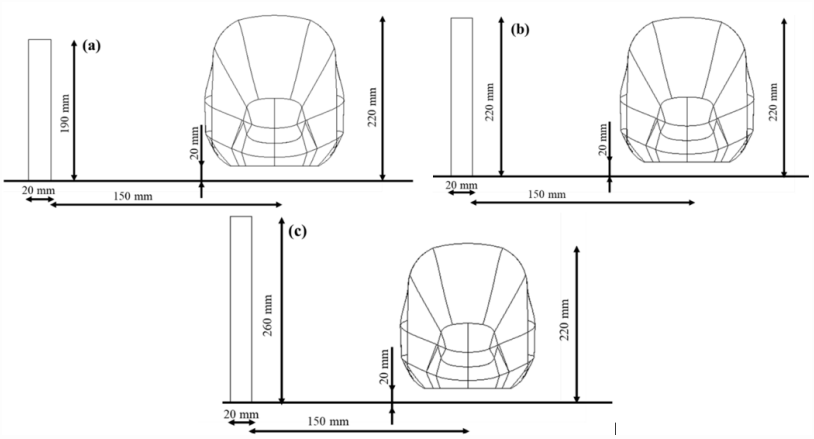

Fig. 2 Variations in the height of windbreak (a) height of 190 mm, (b) height of 220 mm, (c) height of 260 mm

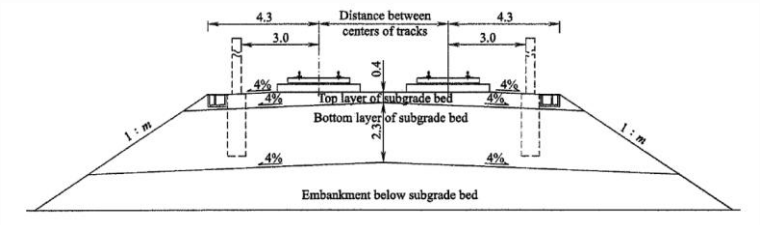

Fig. 3 Dimensions of *embankment* infrastructure in Indonesia

The geometry of the windbreak is designed with 3 height variations, with the train's height as the reference. All these heights are selected to assess the protective effect of the windbreak on the train. As shown in Fig. 2, windbreak (a) has a height of 3.8 m, windbreak (b) has a height of 4.4 m, and windbreak (c) has a height of 5.2 m. For the thickness and length of the windbreak, based on Indonesia's embankment

e-ISSN 2623-0313
p-ISSN 3032-1972

infrastructure conditions, which is 0.4 m, the distance to the train is 3 m. This dimension is determined by the dimensions of embankment infrastructure in Indonesia, as shown in Fig. 3.

The last step is to assemble the boundary condition. Inside the boundary condition, there is a CR400AF train and windbreak infrastructure. As shown in Fig. 4, the train's length, L, is 79.4 m. The scheme is consistent with the research by Yang et al. (2019). Pressure-far field boundary is used as an outer boundary of the atmosphere field, where the pressure gauge is 0 Pa. Pressure Far-Field is also used as an inlet to simulate wind conditions with inputs in the form of Mach numbers and flow directions in the simulation.

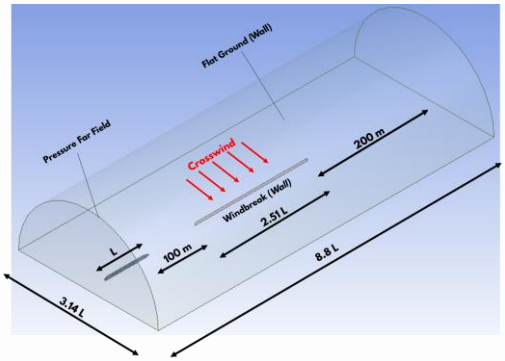

Fig. 4 Geometry assembly for simulation

Mesh System

The assembly was grouped up into two zones, namely, the dynamic zone and the static zone. To realize the flow field data between two regions, interface pairs were used in this simulation. Dynamic zones consist of the CR400AF model and the air near the train. The environment, like the windbreak and boundary, would be grouped into a static zone. The dynamic layering mesh method was performed to realize relative motion between the ground and the train (Deng et al. 2019b, 2020; Yang et al. 2019). The train's speed (Vt) was generalized using mesh motion in the dynamic zones.

In this simulation, an element size of 0.06 m was used. This study also used adaptive sizing with a default value of 1.6×10^{-4} to shorten simulation time. Moreover, body sizing was added to the dynamic zone geometry. This body sizing was used to reduce the mesh size in the dynamic zone region, since the mesh around the train area requires higher quality. In this simulation, the body sizing used is 0.02 m for dynamic zone geometry. The inflation method was applied to the walls of the train, with a total of 8 layers (Yang et al., 2019). Multizone was used in static zone geometry. The static zone uses a multizone with a hexa-mesh shape in a structured section and a free-mesh type. In the dynamic zone, a train geometry is used with the tetrahedron method because the geometry is quite complex. The results of the simulation meshing are shown in Fig. 5. Among the methods above, the skewness metric score was average at 0.23.

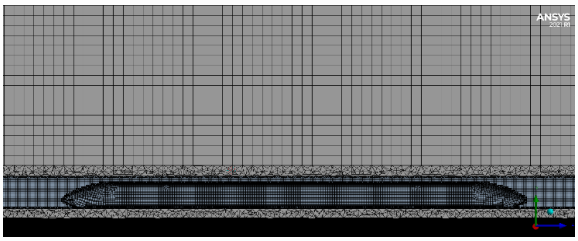

Fig. 5 Simulation mesh

Governing Equation and Solution Scheme

The Mach number (Ma) of the flow field around the HST is less than 0.3, and the Reynolds number is greater than 106. As a result, the flow field in this study is unsteady, turbulent, and incompressible. Due to their requirements for higher grid resolution and a shorter time step in the study of flow structure evolution, large eddy simulation (LES) and detached eddy simulation (DES) typically result in low computational efficiency, making it difficult to complete the work described in this study. Furthermore, the Reynolds-averaged Navier-Stokes (RANS) equations turbulence model is frequently used to simulate flow configurations comparable to those in this study.

The two-equation model, namely the k-ε and k-ω model, is the most popular. In contrast, the k-ε model accurately predicts locations far from boundaries, while the k-ω model accurately predicts locations close to walls, both of which depend on the Y+. In this study, the k-ω model is used as the turbulence model; it is a SST $k-\varepsilon$ model. This modeling aims to combine the advantages of the k-ε and k-ω equations. Where in the zone near the wall, using the k-ω equation, and in the flow far from the wall, using the k-ε equation.

The continuity equation and the momentum conservation equation are part of the governing equations (Navier-Stokes equations). There is no energy conservation equation, since the flow field in this study is assumed incompressible.

$$\frac{\partial \rho}{\partial t} + \frac{\partial}{\partial x_i}(\rho u_i) = 0 \quad (1)$$

$$\frac{\partial}{\partial t}(\rho u_i) + \frac{\partial}{\partial x_j}(\rho u_i u_j) = -\frac{\delta \rho}{\delta x_i} + \frac{\partial \sigma_{ij}}{\partial x_j} + \frac{\partial}{\partial x_j}(-\rho u_i' u_j') \quad (2)$$

e-ISSN 2623-0313
p-ISSN 3032-1972

The simulation will be carried out using a transient method, in which the train moves along the track without a windbreak until it completely passes the windbreak construction.The simulation will be carried out with a train speed of 350 km/h with a crosswind speed of 25 m/s. The result of this setup is to obtain three aerodynamic coefficients and a pressure contour from the time the train enters the windbreak area until it exits. The mesh motion method is used to define a dynamic zone moving at a speed of 350 km/h or 97.2 m/s with the direction of the z axis. Crosswind speed is entered in the boundary condition, that is, in the pressure-far field at a speed of 0.072 Mach with the direction of the x-axis.

To model the train's motion relative to the ground, a dynamic mesh method, namely layering, is used. The concept of sliding mesh can be applied when there is an interface (fluid will still flow) as a barrier between the static and dynamic zones, as well as when using mesh motion and dynamic mesh. In the simulation, the length of the train line is 27 m, so at a speed of 97.2 m/s, the train will take 0.28 seconds to reach the end of the boundary. The time step size used is 1×10^{-3} s. Based on Yang et al. (2019), high-speed train research using a time step size of up to 7×10^{-3} s. Therefore, the number of time steps required is 275, with 20 iterations per time step.

Calculation of Aerodynamic Coefficient

The distributions of pressure and shear stress on an object's surface are the only two basic sources that can account for all aerodynamic forces and moments acting on an object (Anderson, 2010). The ensuing aerodynamic forces and moments on the item are caused by the distribution of pressure and shear stress throughout its whole surface (Anderson, 2010). Train experiences aerodynamic loads due to normal voltage and tangential stress to its surface when moving under crosswind conditions (Ishak et.al., 2019). These stresses give rise to the resulting load components, which are usually expressed in a non-dimensional form through the coefficients of force, and the aerodynamic moments are drag, lift, side, rolling moment, yawing moment, and pitching moment.

Since aerodynamic coefficients have been used as the outcome parameter in numerous studies on the impact of crosswind on train speed (Deng et al., 2020; Deng et al., 2019, Niu et al., 2017, Suzuki et al., 2003), this study will also use aerodynamic coefficients to analyse the phenomena that occur on the track with windbreak as shown in Table 1. In this study, only look for and analyze 3 aerodynamic coefficients, these coefficients are drag force(F_D), lift force, (F_L)and rolling moment(R_{RM}). The yawing and pitching moments were not analyzed because they were less relevant to the actual conditions, namely, they were not based on a single point and had a small impact on the risk of the train overturning.

Table 1 Aerodynamics coefficient equation

Aerodynamic Coefficients	Equation Formula
Side Force (C_s)	$C_s = \frac{F_s}{\frac{1}{2}\rho V_A{}^2 A_{SIDE}}$
Lift Force (C_L)	$C_L = \frac{F_L}{\frac{1}{2}\rho V_A{}^2 A_{SIDE}}$
Drag Force (C_D)	$C_D = \frac{F_D}{\frac{1}{2}\rho V_A{}^2 A_{SIDE}}$
Rolling Moment (C_{RM})	$C_{RM} = \frac{R_{RM}}{\frac{1}{2}\rho V_A{}^2 A_{SIDE} h}$
Yawing Moment (C_{YM})	$C_{YM} = \frac{R_{YM}}{\frac{1}{2}\rho V_A{}^2 A_{SIDE} h}$
Pitching Moment (C_{PM})	$C_{PM} = \frac{R_{PM}}{\frac{1}{2}\rho V_A{}^2 A_{SIDE} h}$

e-ISSN 2623-0313
p-ISSN 3032-1972

Verification of Simulation Setup

The simulation setup used in this study was also used by Yang et al. (2019). In this study, the CRH3 high-speed train was used, traveling at 250 km/h. For quantitative verification of the HST based on wind-tunnel testing, Dorigatti et al. showed that the static and moving results are similar at a specific wind angle and under relatively stable aerodynamic conditions. Followed by verification based on Schober's static ICE3 train test because the outer shape of the CRH3 train is the same as that of the ICE3 train. The results showed that the remaining values are in line with the test results, with the difference remaining around 10%. For qualitative verification, the vortices structure in the two cases has good consistency in terms of distribution position and shape, according to Krajnovic's LES approach. The numerical results in this work are reliable, as shown by quantitative and qualitative comparisons with similar outcomes reported by other researchers.

This study adapts the boundary conditions and simulation parameters, along with the dimensions of the windbreak and high-speed train, to the conditions in Embankment Indonesia. Simplification was also performed on the simulation's size, which was scaled to 1:20. The scaling did not have a significant effect on the high-speed train simulation, according to the study by Niu et al. (2015).

RESULTS AND DISCUSSIONS

The aerodynamic coefficient is the output obtained and will be analyzed in this study. As explained in the previous chapter, three aerodynamic loads result from the simulation: the coefficient of lift, the rolling moment, and the drag force. The drag force is recalculated to obtain the drag coefficient. In this section, an analysis of the aerodynamic coefficient is carried out when there are three variations in the height of the windbreak. During analysis, the graph will be given a boundary line and a region marker to show the train's position in the simulation. Table 2 shows the detailed time steps when the train conditions pass through the windbreak track.

Table 2 Time step of the train position

Time Step	Train Position
56	The head of the train begins to enter the windbreak track
96 – 159	The full body of the train is already inside the windbreak track
160	The head of the train begins to exit the windbreak track
200	The full body of the train is already outside the windbreak track

In Figs. 6-8, the trend graph is generated from the aerodynamic coefficients along the simulation route. Here are some key points for each graph of aerodynamic coefficients.

Fig. 6 shows drag coefficient results. Starting from the position of the initial train until it has begun to enter the windbreak track, the value of the drag coefficient is around (C_d) = 0.19 – 0.27. Furthermore, when the head of the train has begun to enter the track with a windbreak, there is a sudden decrease, so that the value of Cd drops to about 0.21. At time step 148, the drag coefficient values reach global maxima of 0.32 (190 mm windbreak), 0.34 (220 mm windbreak), and 0.35 (260 mm windbreak). The trend is that the drag coefficient increases along the windbreak track. This may be due to the complex flow during the train in that position.

The average values of the drag coefficient variations are 0.286, 0.289, and 0.291, respectively. It means the average drag coefficient will increase further as the height of the windbreak increases.

e-ISSN 2623-0313
p-ISSN 3032-1972

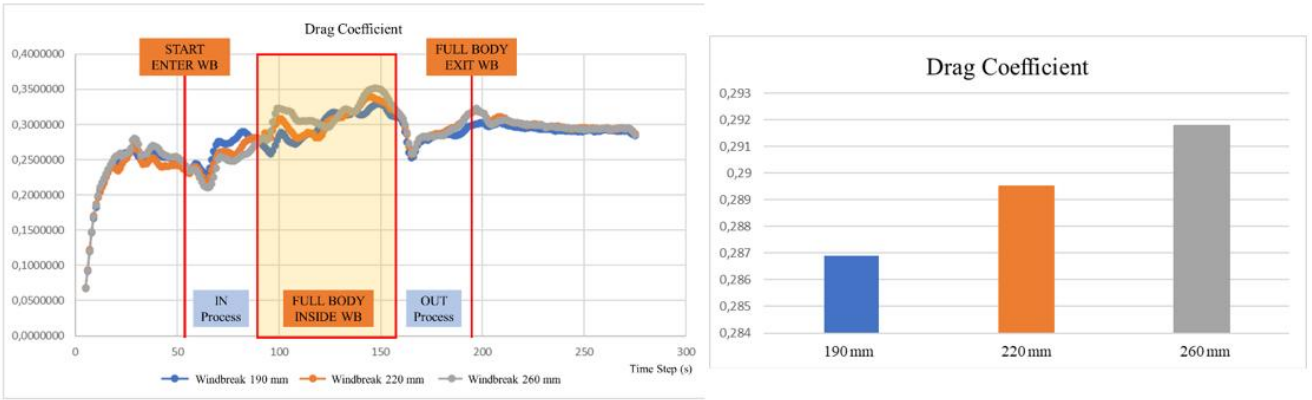

(a) Drag coefficient graph with windbreak height variation

(b) Average drag coefficient when the train starts to enter until the exit of the windbreak track

Fig. 6 Simulation result for drag coefficient

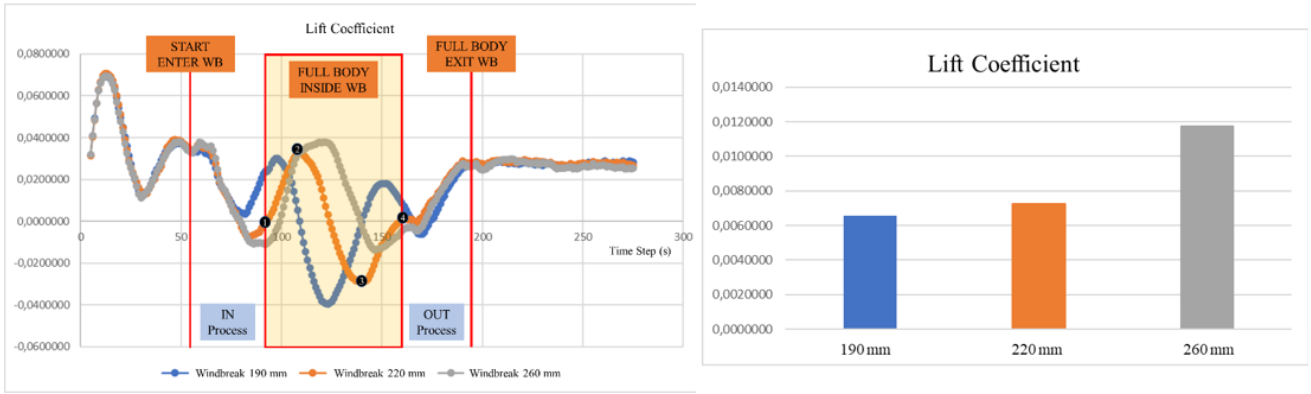

(a) Lift coefficient graph with windbreak height variation

(b) Average lift coefficient when the train starts to enter until the exit of the windbreak track

Fig. 7 Simulation result for lift coefficient

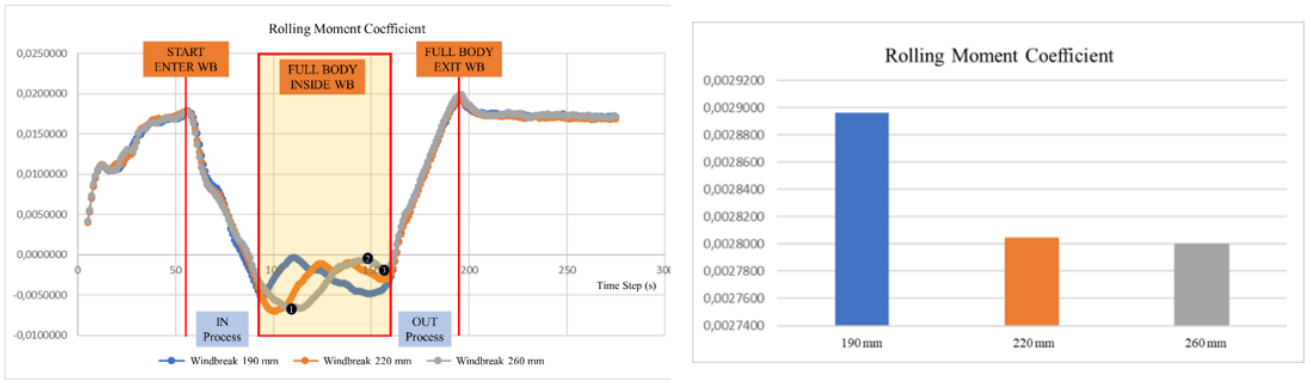

(a) Rolling moment coefficient graph with windbreak height variation

(b) Average rolling moment coefficient when the train starts to enter until the exit of the windbreak track

Fig. 8 Simulation result for rolling moment coefficient

In Fig. 7, the lift coefficient shows several characteristics. Shortly after the train head entered the windbreak track (time step 56), the train lift coefficient decreased slightly to 0.33, then continued to decrease significantly. The minimum value was first located shortly before the full body of the train was inside the windbreak track. The global maximum values of each height variation occur at time steps 97, 109, and 121, with CL values of 0.030, 0.033, and 0.038, respectively. The trend in windbreak height variations follows the same pattern, except that there is a difference in phase and amplitude when the train

e-ISSN 2623-0313
p-ISSN 3032-1972

begins to enter the windbreak track. The average lift coefficient values of the variation are 0.006, 0.007, and 0.011, respectively. This means the average lift coefficient will increase as the windbreak height increases.

Rolling moment characteristics are shown in Fig. 8. The rolling moment coefficient decreases as the train enters the windbreak track or at time step 65, when the train moves 6.3 m from the initial position. The value of the rolling moment coefficient continues to decrease until all train bodies are inside the windbreak track, at which point it becomes -0.004. The trend is similar; it's just that there is a difference in phase and amplitude. It means that the variation in the height of the windbreak in the rolling moment coefficient does not change the characteristic pattern of the trend graph observed in the simulation; it's just that the resulting rolling moment coefficient shifts. The average rolling moment coefficient values of each variation are 0.0029, 0.0028, and 0.0027. It means the average value of the rolling moment coefficient will increase steadily as the height of the windbreak increases.

CONCLUSIONS

Based on the results of simulations and analysis that have been carried out in this study, it can be concluded that when a high-speed train travels on a track with a windbreak in crosswind conditions, it will experience several aerodynamic phenomena as follows:

- The addition of windbreak infrastructure on the track with a crosswind has a significant influence on the three aerodynamic coefficients (drag, lift, and rolling moment). These three aerodynamic coefficients will decrease significantly as the train enters the windbreaker track.
- The IN process has greater fluctuations in aerodynamic load compared to the OUT process. This happens because, when the windbreak exit process allows the vortex on the leeward side of the train to be destroyed and disturbed by the relative motion between the train and the windbreak, a more complex vortex forms on both sides of the train.
- In the variations in windbreak heights of 190 mm, 220 mm, and 260 mm, all three have the same trend of aerodynamic coefficient values; there is only a difference in phase and amplitude when the train is fully inside the windbreak track. The higher the windbreak, the lower the average value of the rolling moment coefficient, while the drag and lift coefficients will be smaller.
    - At the drag coefficient, the highest average value is at a windbreak variation of 260 mm height with a value of $C_D = 0.29$. While the lowest average value is at a height of 190 mm, with a value of $C_D = 0.28$
    - At the lift coefficient, the highest average value is at a windbreak variation of 260 mm height with a value of $C_L = 0.011$. While the lowest average value is at a height of 190 mm, with a value of $C_L = 0.006$
    - At the rolling moment coefficient, the highest average value is at a windbreaker variation of 190 mm height with a value of $C_{RM} = 0.0028$. While the lowest average value is at a height of 260 mm, with a value of $C_{RM} = 0.0027$

ACKNOWLEDGMENTS

The authors gratefully acknowledge the support for computational facilities from the Fluid Mechanics Laboratory, Department of Mechanical Engineering, Faculty of Engineering, Universitas Indonesia.

REFERENCES

Baker, C. (2013). A framework for the consideration of the effects of crosswinds on trains. Journal of Wind Engineering and Industrial Aerodynamics, 123, 130–142.

Baker, C. (2014). A review of train aerodynamics Part 1 – Fundamentals. The Aeronautical Journal (1968), 118(1201), 201-228.

Baker, C. (2014). A review of train aerodynamics Part 2 – Applications. The Aeronautical Journal (1968), 118(1202), 345-382.

Cheng, S.Y., Tsubokura, M., Nakashima, T., Nouzawa, T., Okada, Y., 2011. A numerical analysis of transient flow past road vehicles subjected to pitching oscillation. J. Wind Eng. Ind. Aerodyn. 99, 511-522.

Deng, E., Yang, W., He, X., Ye, Y., Zhu, Z., & Wang, A. (2020). Transient aerodynamic performance of high-speed trains when passing through an infrastructure consisting of tunnel–bridge–tunnel under crosswind. Tunnelling and Underground Space Technology, 102, 103440.

Deng, E., Yang, W., He, X., Zhu, Z., Wang, H., Wang, Y., ... & Zhou, L. (2021). Aerodynamic response of high-speed trains under crosswind in a bridge-tunnel section with or without a wind barrier. Journal of Wind Engineering and Industrial Aerodynamics, 210, 104502.

e-ISSN 2623-0313
p-ISSN 3032-1972

Deng, E., Yang, W., Lei, M., Zhu, Z., & Zhang, P. (2019). Aerodynamic loads and traffic safety of high-speed trains when passing through two windproof facilities under crosswind: A comparative study. Engineering Structures, 188, 320-339.

Guo, Z., Liu, T., Chen, Z., Liu, Z., Monzer, A., & Sheridan, J. (2020). Study of the flow around railway embankment of different heights with and without trains. Journal of Wind Engineering and Industrial Aerodynamics, 202, 104203.

Hashmi, S. A., Hemida, H., & Soper, D. (2019). Wind tunnel testing on a train model subjected to crosswinds with different windbreak walls. Journal of Wind Engineering and Industrial Aerodynamics, 195, 104013.

Ishak, I. A., Ali, M. S. M., Sakri, F. M., Zulkifli, F. H., Darlis, N., Mahmudin, R., ... & Khalid, A. (2019). Aerodynamic Characteristics Around a Generic Train Moving on Different Embankments under the Influence of Crosswind. Journal of Advanced Research in Fluid Mechanics and Thermal Sciences, 61(1), 106-128.

KCIC, “Jakarta - Bandung Fast Train Infrastructure Development,” Jakarta: KCIC, 2018.

Liu, D., Lu, Z., Zhong, M., Cao, T., Chen, D., & Xiong, Y. (2018). Measurements of car-body lateral vibration induced by high-speed trains negotiating complex terrain sections under strong wind conditions. Vehicle System Dynamics, 56(2), 173-189.

Liu, T., Chen, Z., Zhou, X., & Zhang, J. (2018). A CFD analysis of the aerodynamics of a high-speed train passing through a windbreak transition under crosswind. Engineering Applications of Computational Fluid Mechanics, 12(1), 137-151.

Niu, J., Zhou, D., & Liang, X. (2018). Numerical investigation of the aerodynamic characteristics of high-speed trains of different lengths under crosswind with or without windbreaks. Engineering Applications of Computational Fluid Mechanics, 12(1), 195-215.

Shuanbao, Y., Dilong, G., Zhenxu, S., Guowei, Y., & Dawei, C. (2014). Optimization design for aerodynamic elements of high-speed trains. Computers & Fluids, 95, 56-73.

Tomasini, G., Giappino, S., Cheli, F., & Schito, P. (2016). Windbreaks for railway lines: Wind tunnel experimental tests. Proceedings of the Institution of Mechanical Engineers, Part F: Journal of Rail and Rapid Transit, 230(4), 1270-1282.

Wang, D., Chen, D., Li, M., & Liu, G. F. (2016). Research on aerodynamic characteristic for EMU passing by windbreak wall gap under crosswind. Advances in Engineering Research, 113, 19-26.

Yang, A. M., Zhang, C., Li, S. S., Zhang, L., Men, X. J., Kong, F. B., & He, S. Y. (2018). Numerical simulation on the aerodynamic performance of the high-speed train under crosswinds. Journal of Vibroengineering, 20(1), 550-572.

Yang, W., Deng, E., Lei, M., Zhang, P., & Yin, R. (2018). Flow structure and aerodynamic behavior evolution during train entering tunnel with entrance in crosswind. Journal of Wind Engineering and Industrial Aerodynamics, 175, 229-243.

Yang, W., Deng, E., Lei, M., Zhu, Z., & Zhang, P. (2019). Transient aerodynamic performance of high-speed trains when passing through two windproof facilities under crosswinds: A comparative study. Engineering Structures, 188, 729-744.

Yao, Z., Xiao, J., & Jiang, F. (2012). Characteristics of daily extreme-wind gusts along the Lanxin Railway in Xinjiang, China. Aeolian Research, 6, 31-40.

Zhang, L., Zhang, J., Li, T., & Zhang, Y. (2018). A multiobjective aerodynamic optimization design of a high-speed train head under crosswinds. Proceedings of the Institution of Mechanical Engineers, Part F: Journal of Rail and Rapid Transit, 232(3), 895–912